

## Tribomechanical pretreatment of vanadium phosphates: structural and catalytic effects

M. Fait<sup>a</sup>, B. Kubias<sup>a,\*</sup>, H.-J. Eberle<sup>b</sup>, M. Estenfelder<sup>b</sup>, U. Steinike<sup>a</sup> and M. Schneider<sup>a</sup>

<sup>a</sup> *Institut für Angewandte Chemie Berlin-Adlershof e.V., Richard-Willstätter-Strasse 12, D-12489 Berlin, Germany*  
E-mail: b.kubias@aca-berlin.de

<sup>b</sup> *Consortium für Elektrochemische Industrie GmbH, Zielstattstrasse 20, D-81379 München, Germany*

Received 12 July 1999; accepted 25 May 2000

*Dedicated to Professor Dr. Manfred Baerns on the occasion of his 65th birthday*

The influence of the tribomechanical pretreatment of the precursor vanadyl hydrogenphosphate hemihydrate,  $\text{VOHPO}_4 \cdot 0.5\text{H}_2\text{O}$ , prepared in aqueous medium and of the catalyst vanadyl pyrophosphate,  $(\text{VO})_2\text{P}_2\text{O}_7$ , on the structural and catalytic properties of  $(\text{VO})_2\text{P}_2\text{O}_7$  in the oxidation of *n*-butane to maleic anhydride was investigated. Due to the pretreatment the activity and selectivity of the catalyst were markedly increased. The increase in catalytic performance is explained as an effect of the particle size in connection with lattice imperfections.

**Keywords:** vanadium phosphates, real structure, tribomechanical pretreatment, maleic anhydride, butane oxidation

### 1. Introduction

Vanadyl pyrophosphate (VPP),  $(\text{VO})_2\text{P}_2\text{O}_7$ , is well known to be the best suited catalyst for the selective oxidation of *n*-butane to maleic anhydride (MA) [1]. However, in fixed-bed reactors the MA yield reached amounts only to about 60 mol% and the MA productivity of the catalyst is also relatively low compared to other processes of selective oxidation. Therefore, further efforts are necessary to improve both the selectivity and the activity of the VPP catalyst.

A promising new concept to increase the catalytic performance is the tribomechanical pretreatment of the VPP catalyst as well as of the catalyst precursor vanadium hydrogenphosphate hemihydrate (VHP),  $\text{VOHPO}_4 \cdot 0.5\text{H}_2\text{O}$ . The latter can be done due to the fact that imperfections induced in VHP by mechanical pretreatment are transformed into VPP even during calcination [2]. Tribomechanically pretreated catalysts have been described in some papers to become more active and selective in the partial oxidation reaction of *n*-butane to MA. Thus, the pretreatment of a VHP precursor in a not specified mill improved the MA selectivity by 6% at a butane conversion degree of 83% [3]. A rise in the catalytic performance of the VPP catalyst after a tribomechanical pretreatment of the raw material  $\text{V}_2\text{O}_5$ , the VHP precursor and the VPP catalyst, respectively, is also described in [4]. In both papers the improved catalyst performance is explained by an enhanced exposure of the proportion of the (100) plane. In contrast, in [5–7] the increase in MA selectivity is attributed only to an increase in surface area and a generation of fresh and reactive surfaces.

All these investigations do not elucidate beyond any doubt the complex relationships between tribomechanical pretreatment, structural changes, and catalytic performance. If any, only few aspects of the *real* structure of the solids were discussed such as intensity ratios or full widths at half maximum (FWHM) of peaks in the powder diffractograms and exclusively one type of mill was used in all papers cited usually without any details concerning the milling processes. Furthermore, no information was given on the lifetime of the effects enhancing the activity and selectivity of the catalysts.

To answer the question on the possibility to influence the activity and the MA selectivity of the VPP catalysts by milling and to find out the reasons of the expected performance changes the effects of different mills allowing different mechanisms of mechanical pretreatment on the real structure parameters of both the precursor and the catalyst were studied. The activity and selectivity properties of the VPP catalysts activated by these methods were determined after appropriate conditioning in the oxidation of *n*-butane to MA to elucidate relationships between the structural changes and the catalytic properties of the catalysts.

### 2. Experimental

#### 2.1. Preparation, treatment procedures, and catalytic tests

The VHP precursor was prepared by crystallization from an aqueous solution containing  $\text{H}_3\text{PO}_4$  obtained by reduction of  $\text{V}_2\text{O}_5$  with oxalic acid [8]. The tribomechanical pretreatment was carried out in three different laboratory mills

\* To whom correspondence should be addressed.

with different treatment effects: a *pinned disk mill* (1) – impact (63C, Alpine, Germany), a *vibratory disk mill* (2) – shear, pressure (RS1, Retsch, Germany), and a *planetary ball mill* (3) – impact, friction (Pulverisette 7, Fritsch, Germany). Different parameters specific to the respective type of mill (e.g., material of the milling bodies and vessels (zirconia: mill (3), sintered corundum: mill (3), agate: mill (2)), use of additives (water)) and also the time of tribomechanical treatment were varied (cf. table 1 for experimental details). The pretreated VHP materials were pelletized (9 MPa, 0.5 min), crushed and the sieve fractions 1.25–2.5 mm were transformed into VPP in a tubular reactor in a 6% oxygen containing N<sub>2</sub> stream at 400 °C to prevent reduction by small amounts of remaining oxalic acid residues (cf. table 3, samples C0–C3). In one case the precursor was converted first to fresh VPP catalyst which was milled (cf. table 1, sample C4) and after shaping heated in the oxygen containing N<sub>2</sub> stream under the same conditions. In the following conditioning period (18 h, feed gas 1.5 vol% butane in air, constant mass of catalyst samples (5.16 g)) quasi-equilibrated VPP catalysts were generated from the fresh samples. During the catalytic tests MA selectivities were measured in the same tubular reactor depending on residence time and catalyst tempera-

ture and maximum MA yields were determined as the more relevant industrial characteristic.

## 2.2. Characterization

The fresh and pretreated precursor and catalyst specimens were characterized by X-ray powder diffraction (XRPD) using a STADI P (Stoe, Germany) set-up (transmission, Ge primary monochromator, CuK $\alpha$ 1, capillary technique). Data interpretation was carried out using the software Visual X<sup>POW</sup> [9]. For the lattice refinement the PDF files 37-0269 (VHP) and 34-1381 (VPP) [10] were applied. By means of the program PowderCell [11] the orientation factors  $o_l$  which describe the deviation of the crystallite habit from cube-shaped ( $o_l = 1$ ) to plate-shaped ( $o_l < 1$ ) or needle-shaped ( $o_l > 1$ ) were determined. The FWHM,  $\beta_{\text{exp}}$ , for each Bragg reflex was corrected for instrumental broadening,  $\beta_{\text{inst}}$ , yielding the broadening of the diffraction profile,  $\beta_{\text{samp}}$ , given only by the sample without any instrument influences according to  $\beta_{\text{samp}}^2 = \beta_{\text{exp}}^2 - \beta_{\text{inst}}^2$ .  $\beta_{\text{inst}}$  was determined by means of a well-crystallized corundum as an ideal standard sample. The average primary crystallite size  $L$  and the internal microstrain  $\varepsilon$  (cf. table 2) were estimated according to Williamson and Hall [12]. The samples were mixed for the quantitative phase analysis with corundum (1 : 1) as internal standard (assumed 100% crystallinity). Hence, the Rietveld refinement allowed the quantitative determination of the X-ray amorphous fraction of the mechanically treated samples. The secondary particle size was determined by means of a laser particle sizer (Analysette 22, Fritsch, Germany). The specific surface areas were measured according to the BET method by means of a GEMINI III (Micromeritics, USA) from the N<sub>2</sub> physisorption plots.

## 3. Results

### 3.1. Real structure analysis

In the following characteristic real structure data for the VHP precursor and for the VPP catalyst are presented calculated from the XRPD patterns (cf. table 2).

Table 1  
Details of tribomechanical pretreatment procedure.

Sample <sup>a</sup>	Treatment procedure
P0	Untreated
P1	Pinned disk mill (1), peripheral speed 189 ms <sup>-1</sup> , feed rate 7 g min <sup>-1</sup>
P2d	Vibratory disk mill (2), disk mass : powder mass = 23.5 : 1 (dry: 15 g solid), 700 rpm, vessel volume 250 ml, $t = 45$ min
P2w	Vibratory disk mill (2), same conditions as P2d (wet: 15 g solid/9 ml H <sub>2</sub> O)
P3	Planetary ball mill (3), sample mass 16 g, 410 rpm, vessel volume 45 ml, 7 balls, 15 mm $\varnothing$ , corundum grinding set, $t = 60$ min
C4	Planetary ball mill (3), same conditions as P3

<sup>a</sup> P – mechanical treatment of the precursor VOHPO<sub>4</sub>·0.5H<sub>2</sub>O, C – mechanical treatment of the fresh catalyst (VO)<sub>2</sub>P<sub>2</sub>O<sub>7</sub>.

Table 2  
Real structure data<sup>a</sup> of the precursor VOHPO<sub>4</sub>·0.5H<sub>2</sub>O and of the fresh catalyst (VO)<sub>2</sub>P<sub>2</sub>O<sub>7</sub> after tribomechanical precursor treatment in different mills.

Sample	$L$ (Å)	$\varepsilon$ (10 <sup>-3</sup> )	$V$ (Å <sup>3</sup> )	$a$ (Å)	$\Delta a/a_0$ (%)	$b$ (Å)	$\Delta b/b_0$ (%)	$c$ (Å)	$\Delta c/c_0$ (%)
P0	1594	0.2	406.3(1)	7.421(1)	–	9.606(1)	–	5.699(1)	–
P1	1556	0.3	406.1(1)	7.421(1)	0.00	9.606(1)	0.00	5.697(1)	0.00
P2d	1351	0.5	405.5(1)	7.419(1)	–0.03	9.601(2)	–0.05	5.693(1)	–0.11
P2w	1865	0.2	405.3(1)	7.417(1)	–0.05	9.599(2)	–0.07	5.692(1)	–0.12
P3	819	0.9	404.9(2)	7.408(2)	–0.18	9.601(3)	–0.05	5.693(2)	–0.11
C0	65	13.2	1271.6(2)	9.74(1)	–	7.81(2)	–	16.72(3)	–
C2d	41	19.8	1238.6(1)	9.69(3)	–0.51	7.73(3)	–1.02	16.55(5)	–1.02
C2w	88	8.4	1236.0(6)	9.61(1)	–1.33	7.80(1)	–1.28	16.51(3)	–1.26
C3	45	14.4	1110.5(3)	8.868(5)	–8.95	7.594(4)	–2.77	16.49(1)	–1.38

<sup>a</sup> Primary crystallite size  $L$ , internal microstrain  $\varepsilon$ , unit cell volume  $V$ , lattice constants, and relative change of the lattice constants referring to untreated samples  $\Delta a/a_0$ ,  $\Delta b/b_0$ ,  $\Delta c/c_0$ .

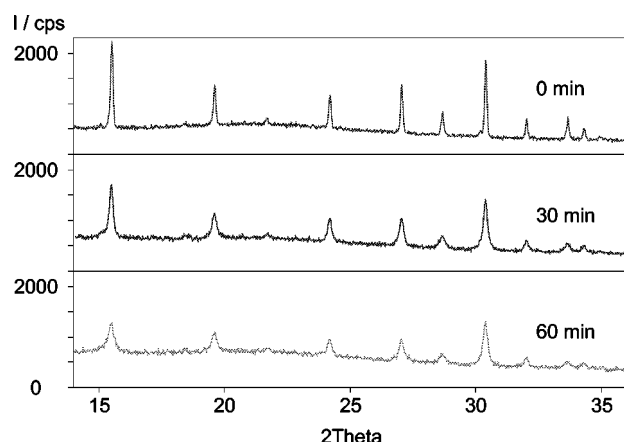


Figure 1. Powder patterns of  $\text{VOHPO}_4 \cdot 0.5\text{H}_2\text{O}$  in dependence on time of tribomechanical treatment in the planetary ball mill (3) with a zirconia grinding set.

### 3.1.1. Real structure of the VHP precursor

A typical example for the changes of the XRPD patterns during the process of milling is depicted in figure 1. It reveals that increasing milling time results in three different effects: (I) a decrease in integral intensity, (II) an increase in the FWHM, and (III) an increase in underground. From the effects (I) and (III) the X-ray amorphous fractions were estimated to increase by about 25% for the material which was mechanically treated in the planetary ball mill (3) for 30 and 60 min, respectively. The relationships between the primary crystallite size calculated from FWHM and the time of the tribomechanical treatment in the same mill (3) are illustrated in figure 2(a). After 9 min the primary crystallite size diminished to a value of about 30% of the original crystallite size whereas a prolonged treatment caused only small changes. The so-called milling equilibrium is reached at about 20 min. Qualitatively this result is in a good agreement with the secondary particle size measured by means of the laser particle sizer mentioned above (cf. figure 2(b)). As figure 2(a) demonstrates, the use of different grinding sets in the mill (3) caused only little differences of the primary crystallite sizes under the treatment conditions chosen.

The effects of the VHP pretreatment in different mills on primary crystallite size, internal microstrain, and unit cell volume and lattice constants, respectively, are summarized in table 2 (samples P0–P3). In contrast to the treatment in mill (1) which caused no changes in the VHP structure (sample P1), the tribomechanical treatment in the mills (2) and (3) resulted in changes of the real structure parameters mentioned with different extent. The primary crystallite size was reduced from 1594 Å (sample P0) to 1351 Å (sample P2d) and 819 Å (sample P3) in the case of the dry milling in the mills (2) and (3), respectively, whereas the “wet treatment” in the mill (2) in the presence of water resulted in an increase in crystallite size to 1865 Å (sample P2w). That is, the wet milling led to grain growing by agglomeration in contrast to the dry milling effecting the comminution. Analogously to the changes of the crystallite sizes but with opposite sign dry milling increased the mi-

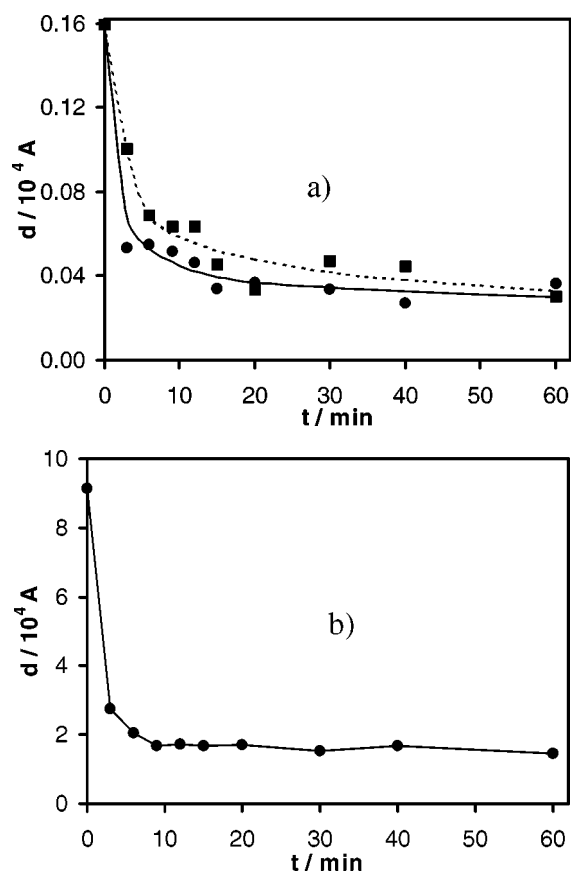


Figure 2. Primary particle size calculated from XRPD experiments (a) and secondary particle size measured with a laser particle sizer (b) of tribomechanically treated  $\text{VOHPO}_4 \cdot 0.5\text{H}_2\text{O}$  vs. time of mechanical treatment using different grinding sets (treatment procedure: planetary ball mill (3), grinding set: zirconia, sintered corundum).

crostrain from  $0.2 \times 10^{-3}$  to  $0.5 \times 10^{-3}$  (sample P2d) and to  $0.9 \times 10^{-3}$  (sample P3), respectively. In contrast, the wet treatment in mill (3) caused no change in microstrain due to water present which is assumed to influence some of the properties of the solid (e.g., decrease in surface energy (Rehbinder effect [13])).

In any case the unit cell volumes were diminished due to the milling procedures in agreement with [2]. The largest lattice contraction indicated by a decrease in the unit cell volume from 406.3 to 404.9 Å<sup>3</sup> was found in the case of the treatment in mill (3) (sample P3). In contrast to the [010] lattice constants which remained constant within the margin of error, the [001] lattice constants were diminished by 0.11–0.12% (samples P2d, P2w, and P3, respectively) due to the tribomechanical effects of both the mill (2) and the mill (3). This finding is explained by the layered VHP structure which is built up of separate sheets of interlinked  $\text{VO}_6$  octahedra and  $\text{PO}_4$  tetrahedra held together by a tight network of hydrogen bonds (cf. figure 3) [14]. The weak hydrogen bonds should be deformed more easily by forces effecting along the [001] direction (*c* axis) than the rigid  $\text{VO}_6/\text{PO}_4$  framework. In addition to the lattice contraction in the [001] direction the treatment in the mill (3) resulted in a marked decrease in the lattice constants in the direction

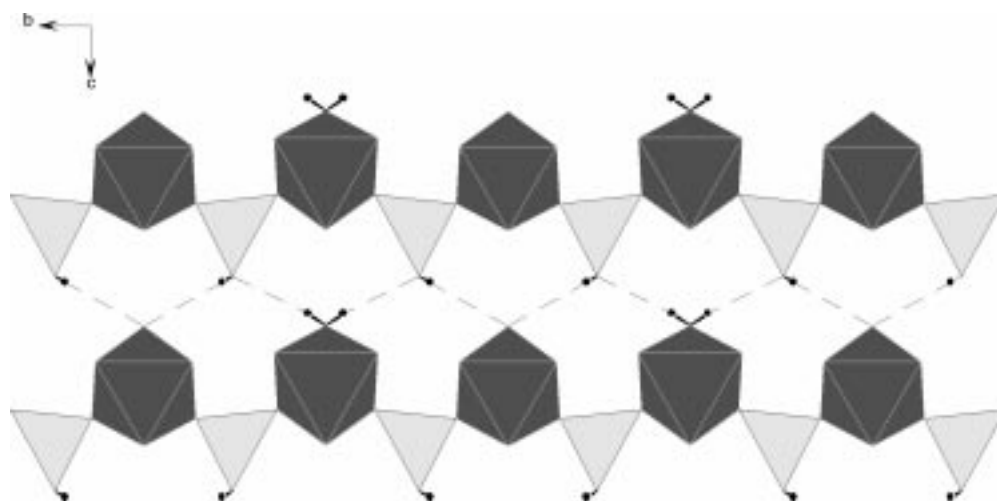


Figure 3. Layered structure of  $\text{VOHPO}_4 \cdot 0.5\text{H}_2\text{O}$  with hydrogen bonds (---) (● are hydrogen atoms) interconnecting the separate sheets built up of  $\text{VO}_6$  octahedra (dark) and  $\text{PO}_4$  tetrahedra (light), view along  $[100]$  direction.

of the  $a$  axis (0.18%, sample P3; no significant changes in the direction of  $b$ ) due to the effect of the high-energy input exerted by ball milling [15].

The calculated orientation factors  $o_1$  of all samples remained constant at  $1.00 \pm 0.02$  which reveals that the cube-shaped crystallite habit of the precursor prepared from aqueous solution did not change during the treatment in the different mills used. This result was confirmed by scanning electron micrographs which showed isometric formed VHP crystallites.

### 3.1.2. Real structure of the fresh VPP catalyst

Compared with their milled precursor counterparts the fresh catalyst specimens exhibited a drastically diminished primary particle size and a strong increased internal micro-strain which is the biggest for sample C2d ( $19.8 \times 10^{-3}$ ). The treatment in mill (2) (under dry conditions, sample C2d) and mill (3) (sample C3) resulted in the smallest primary crystallite sizes (41 and 45 Å, respectively). Analogously to the VHP samples in any case the VPP unit cell volumes were markedly reduced compared with the unmilled material. However, the ratios of the lattice contraction differ considerably in dependence on the mills used: the treatment in the mill (2) caused a reduction of the unit cell volume of only 2.6–2.8% (samples C2d, C2w), whereas the high-energy ball milling (sample C3) resulted in a decrease in the unit cell volume of 12.7% (from 1271.6 to 1110.5 Å<sup>3</sup>). In contrast to the anisotropic VHP lattice contraction, the VPP cell constants were diminished relatively isotropic by mechanical treatment with the exception of the sample C3 exhibiting a pronounced decrease in the lattice constant  $a$ . (Note that the designations of the lattice constants of VPP and VHP, respectively, differ from each other and they change according to the following relationship: (VHP → VPP),  $a \rightarrow c$ ,  $b \rightarrow a$ ,  $c \rightarrow b$ .) As found for the precursor samples the orientation factors of the C samples remained constant at  $o_1 = 1$ , i.e., the crystallites

of the fresh VPP catalyst samples did not show a preferred orientation, too.

### 3.2. Catalytic tests

In table 3 catalytic properties (columns (b)–(d)) and specific surface areas (column (e)) of the VPP specimens obtained from in various different ways tribomechanically treated precursor samples are compared with the results of the untreated material. To determine the effect of the milling on the initial selectivity the MA selectivities were measured at the low butane conversion degree of 30% (cf. column (b)). The butane conversion degrees as a measure of the catalytic activity and the area-specific rates of butane conversion at 375 °C are listed in column (c). In column (d) the maximum MA yields obtained at butane conversion degrees of 83–88% are summarized as the more interesting data from the viewpoint of industrial application.

The catalytic results revealed a marked increase in MA selectivities by 5% (samples C2w and C3) and in maximum MA yields by 5 mol% (sample C2w) due to the tribomechanical pretreatment of VHP and VPP, respectively. Only the VHP treatment in the pinned disk mill (1) (sample C1) caused no rise in MA yield and no increase in the degree of butane conversion at 375 °C. In contrast, the other specimens exhibited a slight increase in butane conversion degrees with the exception of sample C2w ground under wet conditions. The changes in activity and selectivity measured remained constant for more than 70 h time on stream after the conditioning period.

No difference in MA formation between the samples C3 and C4 which differ in the point in time of mechanical pretreatment (after VHP synthesis and after calcination to the fresh catalyst, respectively) was found within the margins of error. In the case of the sample C4 a more pronounced influence of the milling on the specific surface area was observed compared to the other samples. However, the differences in the specific areas of all treated samples are



Table 3

Catalytic properties and specific surface areas of  $(VO)_2P_2O_7$  catalysts prepared from untreated and tribomechanically pretreated  $VOHPO_4 \cdot 0.5H_2O$  precursors ( $GHSV = 1000 \text{ h}^{-1} = \text{const.}$ ).<sup>a</sup>

(a) Sample	(b) $X_b = 30\%$	(c) $T = 375 \text{ }^\circ\text{C}$		(d) Maximum value		(e) $SA_{\text{BET}}$ ( $\text{m}^2 \text{ g}^{-1}$ )
	$S_{\text{MA}}^b$ (%)	$X_b$ (%)	$r_b$ ( $\mu\text{mol m}^{-2} \text{ h}^{-1}$ )	$Y_{\text{MA}}$ (mol%)	$S_{\text{MA}Y_{\text{MA}}}^c$ (%)	
C0	66	30	13.4	$44 \pm 1$	51	16.0
C1	66	30	15.0	$45 \pm 1$	51	14.3
C2d	69	33	13.3	$48 \pm 1$	55	17.7
C2w	71	26	13.2	$49 \pm 1$	56	14.1
C3	71	32	13.6	$47 \pm 1$	57	15.7
C4	70	38	14.4	$48 \pm 1$	57	18.8

<sup>a</sup>  $S_{\text{MA}}$  – MA selectivity,  $X_b$  – butane conversion degree,  $r_b$  – area-specific rate of butane conversion,  $Y_{\text{MA}}$  – maximum MA yield,  $SA_{\text{BET}}$  – specific surface area.

<sup>b</sup>  $T = 364\text{--}381 \text{ }^\circ\text{C}$ .

<sup>c</sup> At the conditions of the maximum MA yield.

only small and, consequently, the area-specific rates did not change significantly, too.

#### 4. Discussion

From the XRPD investigations it follows that the real structure of the VHP was markedly influenced by the tribomechanical pretreatment in both the vibratory disk mill (2) and the planetary ball mill (3). The observed changes in X-ray amorphous fractions, crystallite sizes, and long-range orders are known in principle as results of a mechanical treatment in mills [16]. However, the different mechanisms of the tribomechanical treatment in the mills used caused very different effects on both the precursor and the catalyst lattice: The high-energy milling in the planetary mill (3) resulted in a stronger lattice compression than the treatment in the vibratory disk mill (2). The unchanged activity of sample C1 corresponds to the fact that the treatment in mill (1) did not cause any detectable changes of the real structure parameters of the precursor. The reason of this finding might be of technical nature (too long distances of the pins at the disks and therefore insufficient contact of the grist with the pins).

The finding that imperfections induced in the VHP lattice by mechanical pretreatment are transformed into the VPP catalyst during the calcination due to a memory effect [2] is confirmed by the results of the catalytic tests of the samples C3 and C4 which were mechanically treated at different points in time of their genesis. The MA selectivities and yields of both catalyst samples are at the same level. Therefore, the results obtained by the treatment of the precursors are valid for the catalyst samples generated from these materials.

With the exception of the samples C1 and C2d an enhancement in catalyst activity was observed due to tribomechanical treatment. This enhancement was especially pronounced in the case of the sample C4 ground by high-energy ball milling. The increased catalyst activities correlate with the decrease in the primary crystallite size (cf.

table 2): the smaller the VPP catalyst crystallite size the higher the catalytic activity. Analogously increasing microstrain is correlated with an increase in catalytic activity. The area-specific rates of the butane conversion do not follow this trend totally. Obviously, there is no simple relationship between the catalytic activities and the magnitude of the surface areas in the case of the mechanically treated VHP and VPP specimens.

Apart from the crystallite size effect, the reason for the decrease in the catalytic activity of sample C2w could be the influence of water present during milling which could have caused an enrichment in phosphorus at the surface analogously to the effect of water vapour on the P:V surface ratio of VPP catalysts under reaction conditions [17].

The improved MA selectivities of the pretreated VPP catalyst samples cannot be explained by catalytic anisotropy: the powder patterns of all of the mechanically treated precursors and catalysts investigated gave no hint to the existence of a preferred orientation which had to be indicated by differences in the orientation factors which remained constant at 1 in any case. This is in agreement with the results of Shima et al. [6], who ground a VPP catalyst in the presence of isobutanol and found a marked increase in MA yields without any correlation between the proportion of exposed (100) planes of the VPP crystals and the catalytic selectivity before and after milling. Furthermore, as shown above, the use of different mills exerting different mechanisms of treatment (impact, friction, pressure, shear) caused the same increases in MA selectivities within the margins of error. This may also be seen as an argument that catalytic anisotropy cannot play a role in the catalytic action of VPP catalysts at least in the case of the catalysts prepared from aqueous medium. The increase in MA selectivity caused by milling of the VHP precursor or of the VPP catalyst seems to be more likely a consequence of induced lattice imperfections possibly connected with a particle size effect. As it follows from the MA selectivities of the samples at a butane conversion degree of 30% (cf. table 3) these phenomena influence the initial MA selec-

tivities (i.e., the ratio of the rates of the selective and the sum of total and selective oxidation reactions of butane) more than the ability of the catalyst to oxidize MA formed. To confirm this and to elucidate further relationships between the catalytic performance and the structure of the VPP catalyst in the butane oxidation work is in progress to extend the conclusions drawn on VPP catalysts prepared from alcoholic media.

### Acknowledgement

This work was supported by the Bundesministerium fuer Bildung und Forschung (contract No. 03C02735). The authors are gratefully to E. Thiede, Dr. D. Groke, Dr. H.-P. Hennig, Dr. U. Bentrup, U. Gerber and W. Hopfe for experimental assistance.

### References

- [1] G. Centi, *Catal. Today* 16 (1993) 5.
- [2] U. Steinike, B. Müller and A. Martin, *Mater. Sci. Forum* (1999), in press.
- [3] H.S. Horowitz, C.M. Blackstone, A.W. Sleight and G. Teufer, *Appl. Catal.* 38 (1988) 193.
- [4] V.A. Zazhigalov, J. Haber, J. Stoch, A.I. Kharlamov, L.V. Bogutskya, I.V. Bacherikova and A. Kowal, *Stud. Surf. Sci. Catal.* 110 (1997) 337.
- [5] C.B. Hanson and C.R. Harrison, EP 0098065A2 (1984).
- [6] K. Shima, M. Ito, M. Murayama and M. Hatano, *Sci. Technol. Catal.* 92 (1995) 355.
- [7] G.J. Hutchings and R. Higgins, *Appl. Catal. A* 154 (1997) 103.
- [8] T. Götze, H. Wolf, B. Kubias and M. Meisel, *Chem. Technol. Eur.* 49 (1997) 62.
- [9] Visual X<sup>POW</sup> V. 2.27, Stoe Darmstadt, Germany (1994).
- [10] JCPDS Powder Diffraction File, Powder Diffraction File of the Joint Committee on Powder Diffraction Standards, published by the International Centre for Diffraction Data, 1601 Park Lane, Swarthmore, USA, PA 19081.
- [11] W. Kraus and G. Nolze, *PowderCell* V. 2.1 (1999).
- [12] G.K. Williamson and W.H. Hall, *Acta Metall. Mater.* 1 (1953) 22.
- [13] P.A. Reh binder, *Z. Phys.* 72 (1931) 91.
- [14] C.C. Torardi and J.C. Calabrese, *Inorg. Chem.* 23 (1984) 1308.
- [15] C.J.H. Jacobsen, J. Jiang, S. Mørup, B.S. Clausen and H. Topsøe, *Catal. Lett.* 61 (1999) 115.
- [16] G. Heinicke, *Tribochemistry* (Akademie Verlag, Berlin, 1984).
- [17] B. Kubias, F. Richter, H. Papp, A. Krepel and A. Kretschmer, *Stud. Surf. Sci. Catal.* 110 (1997) 461.